

Theory of microphase separation on Side-Chain Liquid-Crystalline Polymers with flexible spacers

Marcela Hernández^{1,2} and Harry Westfahl Jr.²

¹*Instituto de Física “Gleb Wataghin”, Universidade Estadual de Campinas, Caixa Postal 6165, Campinas SP 13083-970, Brazil*

²*Laboratório Nacional de Luz Síncrotron-ABTLuS, Caixa Postal 6192, Campinas, SP 13043-090, Brazil*

We model a melt of monodisperse side-chain liquid crystalline polymers as a melt of comb copolymers in which the side groups are rod-coil diblock copolymers. We consider both excluded volume and Maier-Saupe interactions. The first acts among any pair of segments while the latter acts only between rods. Using a free energy functional calculated from this microscopic model, we study the spinodal stability of the isotropic phase against density and orientational fluctuations. The phase diagram obtained in this way predicts nematic and smectic instabilities as well as the existence of microphases or phases with modulated wave vector but without nematic ordering. Such microphases are the result of the competition between the incompatibility among the blocks and the connectivity constraints imposed by the spacer and the backbone. Also the effects of the polymerization degree and structural conformation of the monomeric units on the phase behavior of the side-chain liquid crystalline polymers are studied.

I. INTRODUCTION

Side-chain liquid crystalline polymers (SCLCP) are comb copolymers composed of a long main chain backbone with elongated rigid side chains regularly attached through flexible spacers chain (schematic representation on figure 1). Despite their high viscosity, which can be two orders of magnitude higher than monomeric liquid crystals, SCLCP are good candidates to storage information by locking oriented structures into glassy states [1].

These interesting complexes can be thought of as supramolecular polymers of rod-coil diblock copolymers. In rod-coil diblock copolymers the incompatibility between blocks competes against their connectivity leading to a frustration of the macroscopic phase separation. This competition, together with the tendency of the rod segments to align with each other, results in a remarkably rich variety of microphase geometries[2, 3]. Such patterns are characterized by alternating regions of each block with different collective orientations of the rods[4]. The main difference between the rod-coil diblock copolymers and the SCLCP is the introduction of additional correlations among the rigid molecules brought by their linking through the backbone[5][6]. Based on the accumulated theoretical and experimental knowledge on rod-coil diblock copolymers[3][7][8][9] and comb-like copolymers[10][11][12] it is natural to expect that microphase segregation will also play an important role in SCLCP.

The current experimental and theoretical understanding of the physical properties of liquid crystalline polymers derives from the knowledge on monomeric liquid crystals and their solutions with polymers. In a pioneering work, Vasilenko, Shibaev and Khokhlov [13] developed a model for the SCLCP based on Matheson and Flory [14] lattice theory for chains with rodlike sections.

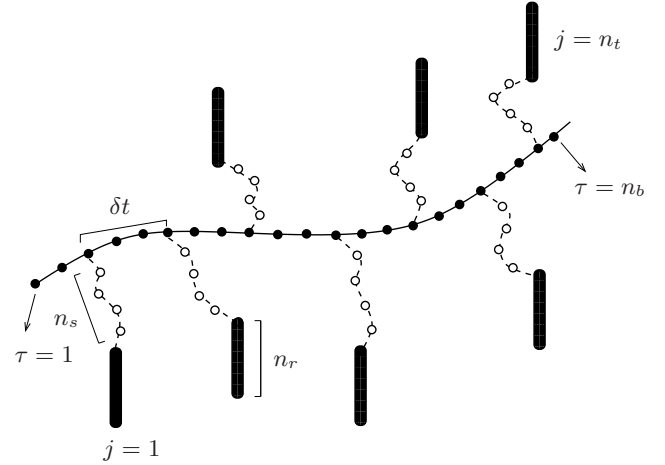


Figure 1: Model for the side chain polymer. The backbone and the spacer are considered as Gaussian chains of n_b and n_s segments respectively while the rigid rods have n_r segments. There are n_t side groups separated by a distance δt along the backbone.

The emergence of thermodynamic phases with complex nematic orderings was then described as a purely entropic effect driven by the main chain flexibility. This model has been later improved by Auriemma, Corradini and Vacatello[15] to better include steric repulsion effects. These theories neglect the Maier-Saupe anisotropic interaction and should be thus valid in cases where Maier-Saupe interaction between segments is negligible when compared to steric repulsion. The study of anisotropic interactions in SCLCP was first introduced by Wang and Warner [16]. Their theory describes the interplay between side-chains and backbone nematic orderings by means of an extension of the Maier-Saupe theory. In this case, the SCLCP melt is treated as a mixture of worm-like

molecules and rigid rods with their own nematic ordering tendencies analogously to the model studied by ten Bosch, Maissa and Sixou [17] for a solution of nematic polymers in liquid crystalline solvents. The Maier-Saupe coupling (MS) between the backbone and the side-chains is introduced through a constant that describes the effective flexibility of the spacer and determines up to which extent the side and main chains tend to be perpendicular. While in the case of a solution of nematic polymers in liquid crystal solvents the MS coupling between the backbone and the side chains is always positive, i.e., tends to align them, in the SCLCP the coupling due to the effective spacer attachment competes against the nematic coupling between the side-chain and the backbone. This yields an effective nematic coupling between the backbone and the side chains which can be either positive or negative, depending on the relative strength of the two terms. In Wang and Warner theory excluded volume interactions are not taken into account. Thus, we should expect it to be valid in the limit where the Maier-Saupe interaction is much stronger than excluded volume interactions. The possibility of microphase separation driven from the competition between the mesogens and the backbone + spacer complex is not considered in the aforementioned theories.

In this paper, along the lines of Holyst and Schick[18] and Reenders and ten Brinke[7], we study the interplay between microphase separation and nematic ordering in SCLCP. We treat an intermediate region where both excluded volume effects and Maier-Saupe interaction are present. We consider that the Maier-Saupe interaction acts only between rods and that the excluded volume effect acts among all monomers. This should be a reasonable approximation when both spacer and backbone are flexible. We model the SCLCP as a comb polymer composed of a backbone and spacer as in reference [10] with rigid rods attached to the tips of the comb teeth. The comb polymer melt is treated as a set of Gaussian chain with Flory-Huggins interaction and Maier-Saupe interaction between rods. The Landau free energy functional is derived and the spinodal stability curves are obtained as function of the SCLCP structural and interaction parameters. Within our formulation the main difference between a rod-coil polymer formed by the spacer and rod and the SCLCP arises from the inter-rod and inter-spacer correlations induced by the connectivity through the backbone. Since our main aim in this paper is to study the microphase separation instabilities we will not consider here the nematic ordering of the backbone.

II. THE MODEL

We model a melt of monodisperse n_p side-chain polymers with N segments of statistical length b as a chain of n_t rod-coil copolymers regularly attached to a backbone as schematically represented on figure 1. The backbone and the spacer (i.e., the coil part of the rod-coil copoly-

mer) are flexible Gaussian chains of n_b and n_s monomers respectively. The rigid rods are made of n_r segments linearly arranged along a fixed direction. It is useful to define the volume fraction of the rods, $f_r = \frac{n_r n_t}{N}$, the volume fraction of the spacers $f_s = \frac{n_s n_t}{N}$ and the volume fraction of the backbone segments, $f_t = \frac{n_b}{N}$.

There are two important interactions that we consider in our model. The first one is the steric repulsion between any monomers. The second interaction is the Maier-Saupe potential[19][20] that tends to align the mesogens. We write the interaction Hamiltonian as

$$\beta H_I = \sum_{K \neq K' \in (b,s,r)} \int d\mathbf{x} \epsilon_{KK'} \hat{\phi}_K(\mathbf{x}) \hat{\phi}_{K'}(\mathbf{x}) - \frac{\omega}{2} \int d\mathbf{x} \hat{Q}^{\mu\nu}(\mathbf{x}) \hat{Q}^{\nu\mu}(\mathbf{x}), \quad (1)$$

where K and K' represent the monomer species indexes, i.e, backbone segment, spacer segment or rod segment, while $\epsilon_{KK'}$ and ω are the strength of the interaction potentials. Equation (1) is already written in terms of the volume fractions $\hat{\phi}_K(\mathbf{x})$ and the nematic tensor $\hat{Q}^{\mu\nu}(\mathbf{x})$ of the rods, where the local volume fractions of the species are defined as

$$\hat{\phi}_b(\mathbf{x}) = v_0 \sum_{\alpha=1}^{n_p} \int_0^{n_b} d\tau \delta[\mathbf{x} - \mathbf{X}_\alpha^b(\tau)], \quad (2)$$

$$\hat{\phi}_s(\mathbf{x}) = v_0 \sum_{\alpha=1}^{n_p} \sum_{j=1}^{n_t} \int_0^{n_s} d\tau \delta \left[\mathbf{x} - \mathbf{X}_\alpha^{s,j}(\tau) - \mathbf{X}_\alpha^b \left(\left(j - \frac{1}{2} \right) \delta t \right) \right], \quad (3)$$

$$\hat{\phi}_r(\mathbf{x}) = v_0 \sum_{\alpha=1}^{n_p} \sum_{j=1}^{n_t} \int_0^{n_r} d\tau \delta \left[\mathbf{x} - \mathbf{u}_\alpha^j \tau - \mathbf{X}_\alpha^{s,j}(n_s) - \mathbf{X}_\alpha^b \left(\left(j - \frac{1}{2} \right) \delta t \right) \right], \quad (4)$$

where v_0 is the volume of each segment and j labels the side-group position along the backbone. For the backbone, $\mathbf{X}_\alpha^b(\tau)$ is the curve that describes the conformation of the chain α as a function of τ , which labels the monomers in the chain. For the spacers, separated by $\delta t = \frac{n_b}{n_t}$ segments, $\mathbf{X}_\alpha^{s,j}(\tau)$ describes their conformation starting at position $\mathbf{X}_\alpha^b \left(\left(j - \frac{1}{2} \right) \delta t \right)$ on the backbone. The unit vector \mathbf{u}_α^j defines the orientation of the rod j , connected to the end of the spacer at position $\mathbf{X}_\alpha^{s,j}(n_s) + \mathbf{X}_\alpha^b \left(\left(j - \frac{1}{2} \right) \delta t \right)$.

The nematic tensor of the rods is defined as

$$\hat{Q}^{\mu\nu}(\mathbf{x}) = v_0 \sum_{\alpha=1}^{n_p} \sum_{j=1}^{n_t} \int_0^{n_r} d\tau \left(u_{\mu,\alpha}^j u_{\nu,\alpha}^j - \frac{1}{3} \delta_{\mu\nu} \right)$$

$$\begin{aligned} & \times \delta \left[\mathbf{x} - \mathbf{u}_\alpha^j \tau - \mathbf{X}_\alpha^{s,j} (n_s) \right. \\ & \left. - \mathbf{X}_\alpha^b \left(\left(j - \frac{1}{2} \right) \delta t \right) \right]. \end{aligned} \quad (5)$$

For the sake of simplicity we will consider that the backbone and the spacer are made of the same segments. In this way, they can be described by a single field $\hat{\phi}_c = \hat{\phi}_b + \hat{\phi}_s$.

Following Gupta and Edwards [21] we rewrite the partition function of the entire melt in terms of collective variables $\phi_c, \phi_r, \mathbf{Q}$ as

$$\mathcal{Z} = \int \mathcal{D}\phi_c \int \mathcal{D}\phi_r \int \mathcal{D}\mathbf{Q} e^{-\beta H_I[\phi_c, \phi_r, \mathbf{Q}]} \mathcal{Z}_0[\phi_c, \phi_r, \mathbf{Q}] \quad (6)$$

where \mathcal{Z}_0 is the partition function of independent SCLCP molecules which yields the entropic contribution to the total free energy and is given by

$$\begin{aligned} \mathcal{Z}_0 & \propto \prod_{\alpha=1}^{n_p} \prod_{j=1}^{n_t} \int \mathcal{D}\mathbf{X}_\alpha^b \int \mathcal{D}\mathbf{X}_\alpha^{s,j} \int \mathcal{D}\mathbf{u}_\alpha^j \delta(\phi_c - \hat{\phi}_c) \\ & \times \delta(\phi_r - \hat{\phi}_r) \delta(\mathbf{Q} - \hat{\mathbf{Q}}) \delta(|\mathbf{u}_\alpha^j| - 1) \\ & \times e^{-\beta H_0[\mathbf{x}_\alpha^b, \mathbf{x}_\alpha^{s,j}]}. \end{aligned} \quad (7)$$

The Hamiltonian of unperturbed Gaussian chains, H_0 , is written as

$$\begin{aligned} \beta H_0 & = -\frac{3}{2Nb^2} \left[\int \mathcal{D}\tau \left(\frac{\partial \mathbf{X}_\alpha^b(\tau)}{\partial \tau} \right)^2 \right. \\ & \left. + \int \mathcal{D}\tau \left(\frac{\partial \mathbf{X}_\alpha^{s,j}(\tau)}{\partial \tau} \right)^2 \right]. \end{aligned}$$

As discussed by Shinozaki et al.[10], this assumption of Gaussian statistics for the chains is probably not the more realistic since the chains might be stretched relative to the Gaussian case. Nevertheless, for comb with an evenly spaced teeth and small monomer density, the Gaussian description is still reasonable.

We now use auxiliary fields h_c, h_r and $h_Q^{\mu\nu}$ to express the Dirac deltas in equation (7),

$$\begin{aligned} \mathcal{Z}_0[\phi_c, \phi_r, \mathbf{Q}] & \propto \int \mathcal{D}h_c \int \mathcal{D}h_r \int \mathcal{D}\mathbf{h}_Q e^{-i \int d\mathbf{r} h_c \phi_c} \\ & \times e^{-i \int d\mathbf{r} h_r \phi_r} e^{-i \int d\mathbf{r} h_Q^{\mu\nu} Q^{\mu\nu}} \\ & \times \exp\{-F_1[h_r, h_c, \mathbf{h}_Q]\}, \end{aligned} \quad (8)$$

where

$$\begin{aligned} \exp\{-F_1[h_r, h_c, \mathbf{h}_Q]\} & \equiv \prod_{\alpha=1}^{n_p} \prod_{j=1}^{n_t} \int \mathcal{D}\mathbf{X}_\alpha^b \int \mathcal{D}\mathbf{X}_\alpha^{s,j} \\ & \times \int \mathcal{D}\mathbf{u}_\alpha^j \delta(|\mathbf{u}_\alpha^j| - 1) \\ & \times e^{-\beta H_0[\mathbf{x}_\alpha^b, \mathbf{x}_\alpha^{s,j}]} e^{i \int d\mathbf{r} h_c \hat{\phi}_c} \\ & \times e^{i \int d\mathbf{r} h_r \hat{\phi}_r} e^{i \int d\mathbf{r} h_Q^{\mu\nu} \hat{Q}^{\mu\nu}}. \end{aligned} \quad (9)$$

Following references [21] and [22], the integrals over the auxiliary fields in equation (8) are approximated according to the steepest descent method. We write the entropic contribution to the free energy, $F_1[h_r, h_c, \mathbf{h}_Q]$, as :

$$F_1[h_r, h_c, \mathbf{h}_Q] = \left[h_r h_c h_Q^{\mu\nu} \right] G^{(2)\mu\nu\rho\sigma} \begin{bmatrix} h_r \\ h_c \\ h_Q^{\rho\sigma} \end{bmatrix}, \quad (10)$$

where $G^{(2)\mu\nu\rho\sigma}$ is the matrix of non interacting pair correlation functions :

$$G^{\mu\nu\rho\sigma} = \begin{pmatrix} G_{rr} & G_{rc} & G_{rQ}^{\rho\sigma} \\ G_{cr} & G_{cc} & G_{cQ}^{\rho\sigma} \\ G_{Qr}^{\mu\nu} & G_{Qc}^{\mu\nu} & G_{QQ}^{\mu\nu\rho\sigma} \end{pmatrix}. \quad (11)$$

The non-interacting chains pair correlation functions are given by

$$G_{KK'}(\mathbf{x}, \mathbf{x}') \equiv \left\langle \hat{\phi}_K(\mathbf{x}) \hat{\phi}_{K'}(\mathbf{x}') \right\rangle_0$$

$$G_{KQ}^{\mu\nu}(\mathbf{x}, \mathbf{x}') \equiv \left\langle \hat{\phi}_K(\mathbf{x}) \hat{Q}^{\mu\nu}(\mathbf{x}') \right\rangle_0$$

for $K, K' = r, c$, and

$$G_{QQ}^{\mu\nu, \rho\sigma}(\mathbf{x}, \mathbf{x}') \equiv \left\langle \hat{Q}^{\mu\nu}(\mathbf{x}) \hat{Q}^{\rho\sigma}(\mathbf{x}') \right\rangle_0$$

where $\langle \dots \rangle_0$ means the average over the partition function of the unperturbed Gaussian chains 8 and $\hat{\phi}_K(\mathbf{x})$ and $\hat{Q}^{\mu\nu}(\mathbf{x})$ are defined in equations (2), (3), (4) and (5). We can now expand the total free energy of the system as a function of the order parameters ϕ and \mathbf{Q} following the same procedure as in references [22] and [7]. At this point, we assume that the system is incompressible, i.e.,

$$\phi_c(\mathbf{x}) + \phi_r(\mathbf{x}) = 1, \quad (12)$$

which for $\mathbf{q} \neq 0$ means

$$\phi_{r,\mathbf{q}} = -\phi_{c,\mathbf{q}} \equiv \phi_{\mathbf{q}}.$$

After applying condition in Hamiltonian, the excluded volume interaction term reduces to

$$\chi \int d\mathbf{x} \hat{\phi}(\mathbf{x})^2,$$

where $\chi = \epsilon_{cc} + \epsilon_{rr} - 2\epsilon_{cr}$ is the usual Flory-Huggins parameter[23].

The second order expansion term, which defines the stability limits of the isotropic phase against fluctuations of the order parameters, is given by

$$\mathcal{F}[\phi_{\mathbf{q}}, \mathbf{Q}_{\mathbf{q}}] = \frac{1}{2} \sum_{\mathbf{q}} \left[\phi_{-\mathbf{q}}, Q_{-\mathbf{q}}^{\mu\nu} \right] \Gamma_{\mathbf{q}}^{(2)\mu\nu\rho\sigma} \begin{bmatrix} \phi_{\mathbf{q}} \\ Q_{\mathbf{q}}^{\rho\sigma} \end{bmatrix}. \quad (13)$$

The second order vertex $\Gamma^{(2)\mu\nu\rho\sigma}$ is the inverse of the matrix $G^{\mu\nu\rho\sigma}$, as calculated in references [7] and [24], plus a diagonal matrix that contains the terms for the Flory-Huggins interaction and the Maier-Saupe potential:

$$\Gamma^{(2)\mu\nu\rho\sigma} = [G^{\mu\nu\rho\sigma}]^{-1} - \begin{pmatrix} 2N\chi & 0 \\ 0 & \frac{2N\omega}{3} \end{pmatrix}. \quad (14)$$

This approximation for the second order vertex, known as random phase approximation (RPA) is considered as reasonable for dense mixtures of strongly correlated polymer chains, where the fluctuations are very small [25][26]. The calculation the matrix (14) follows along the same lines of reference [7]. The major difference here is that there are additional correlations between the rods and the spacers attached to the same backbone, in contrast to the rod-coil copolymer studied in reference [7]. For instance, the Fourier transform of the rod-rod correlation function in the SCLCP is given by

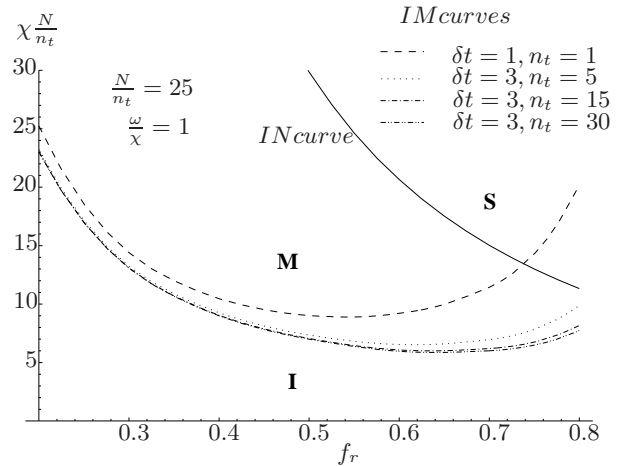
$$G_{rr}(\mathbf{q}) = f_r^2 \left[\frac{1}{n_t} K_{rr}(lq) + e^{-2q^2 R_s^2} F_r(lq)^2 \left(D_{n_t}(qR_b) - \frac{1}{n_t} \right) \right] \quad (15)$$

where, $K_{rr}(x) = \frac{2}{x^2} [\cos(x) - 1 + x Si(x)]$, is the rod-rod correlation function for the rod-coil copolymer studied in reference [7], $F_r(x) = \frac{Si(x)}{x}$ is the form factor of a rod of length l and $D_n(x) = \frac{1}{2n^2} \frac{e^{-x^2} + \sinh\left(\frac{x^2}{n}\right)n-1}{\sinh^2\left(\frac{x^2}{2n}\right)}$ is the Debye function for the backbone. Here we use $l = n_r b$ as the length of the rod and $R_s = \sqrt{\frac{n_s b^2}{6}}$ and $R_b = \sqrt{\frac{n_t b^2}{6}}$ as the gyration radius of the spacer and of the backbone respectively.

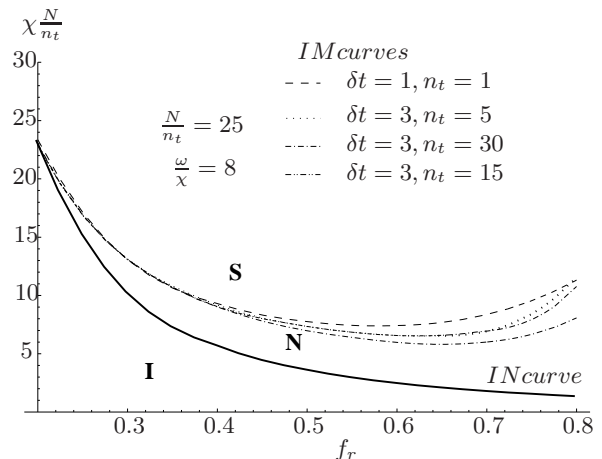
Note that in the limit $n_t = 1$ and $\delta t \rightarrow 0$ the correlation function (15) reduces to the rod-rod correlation function for the rod-coil copolymer studied in reference [7]. In the opposite limit, for $n_t \gg 1$, which is the case of SCLCP the rod-rod correlation function is dominated by the inter-rod correlations within a SCLCP and it is mostly influenced by the backbone and spacer correlations. This is what leads to the main aspect of the physical properties of SCLCP when compared to rod-coil copolymers and to the strong dependence of the mesophases on the structural parameters of the SCLCP [6][1]. The other correlations functions are shown in appendix A.

Also, as done in reference [7], we consider a nematic ordering parallel to the wave vector \mathbf{q} :

$$Q^{\mu\nu}(\mathbf{q}) = Q(\mathbf{q}) \left(\frac{q^\mu q^\nu}{q^2} - \frac{\delta^{\mu\nu}}{3} \right). \quad (16)$$



(a)



(b)

Figure 2: Effect of the polymerization degree and the relation between the Maier-Saupe and Flory-Huggins interactions on the phase diagram for SCLCP for (a) $\frac{\omega}{\chi} = 1$ (b) $\frac{\omega}{\chi} = 8$. The isotropic phase is denoted by “I”, while the microphases, nematic and smectic phases are labeled as “M”, “N” and “S” respectively. The diagrams were calculated for $\frac{N}{n_t} = 25$, different values of n_t and δt as indicated.

III. PHASE BEHAVIOR

A. Stability limits of the isotropic phase: phase diagram

The stability of the isotropic phase against fluctuations of the order parameters is given by the spinodal curve. The roots of the determinant of $\Gamma^{(2)\mu\nu\rho\sigma}$ define an expression for χ as a function of the wave vector q , the structural parameters n_r , n_s , n_t , δt and the ratio between Maier-Saupe and Flory Huggins interactions:

$$\det[\Gamma^{(2)\mu\nu\rho\sigma}] = 0 \rightarrow \chi\left(q, n_r, n_s, n_t, \delta t, \frac{\omega}{\chi}\right). \quad (17)$$

For n_r , n_s , n_t , δt and $\frac{\omega}{\chi}$ fixed, the spinodal curve is determined by the minimization of χ with respect to q . This has been calculated using a program written for Mathematica and available from the authors by request. As discussed in reference [24], if the value q^* that minimizes equation (17) is equal to zero, the isotropic phase is unstable to a nematic phase. If $q^* \neq 0$, then the isotropic phase is unstable against modulations of the volume fraction, which gives raise to microphase separation. On that basis, it is possible to construct a phase diagram that sketches the the transition from an isotropic phase to an ordered stated as a function of the structural parameters of the model. For shortness and simplicity, in this paper we denote as IN the spinodal obtained from the condition $q^* = 0$ and IM the spinodal calculated according to $q^* \neq 0$.

B. Effect of the polymerization degree

In figure 2, we show the effect of the polymerization degree on the phase diagram for two different values of the ratio $\frac{\omega}{\chi}$. In both cases, the phase diagram for $\delta t = 1$, $n_t = 1$ is the same as the rod-coil diblock copolymer phase diagram calculated in reference [7]. The region under the curves corresponds to an isotropic phase, denoted as ‘‘I’’ in the figure. Above them, the phase can be either nematic (N), microphase (M) or smectic (S), which is superposition of the nematic ordering and density modulation. When the Maier-Saupe interaction is of the same order of the Flory-Huggins interaction, i.e. $\frac{\omega}{\chi} = 1$, the phase diagram shows the possibility of having microphase segregation before the transition to a smectic state, like in phase diagram (a) of figure 2. If the value of the ratio $\frac{\omega}{\chi}$ is such that there is no crossing point between the two spinodals, as in phase diagram (b) of figure 2, there is no microsegregation for any volume fraction. This might be attributed to the fact that in this case, the Maier-Saupe interaction is stronger than the Flory-Huggins interaction. Therefore therefore the nematic ordering occurs first than the modulation of the density.

We note that the spinodal curves for the isotropic-nematic instabilities, are given by

$$\omega = \frac{15}{2f_r^2 \left(\frac{N}{n_t}\right)}. \quad (18)$$

This instability line does not depend on the polymerization degree of the SCLCP but only on the ratio $\frac{N}{n_t}$, i.e, the total number of monomers in each rod-coil comb plus δt . This is exactly the same dependence as the case of a single rod-coil studied in reference [7]. It is a consequence of the approximated model we adopted where the rods only interact through the Maier-Saupe coupling among themselves. Since the isotropic-nematic instability occurs at the wave-vector $q = 0$, the inter-rod coupling along a

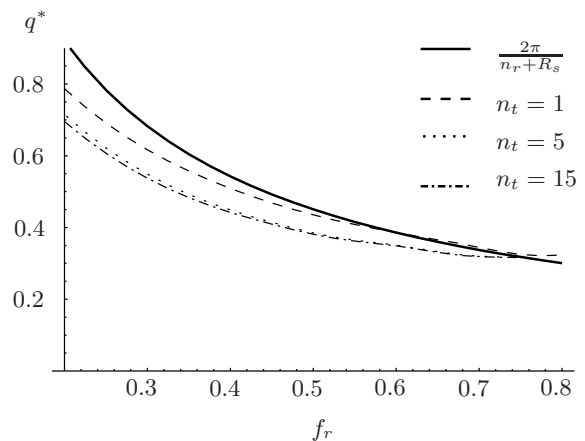


Figure 3: Value of the wave vector q^* that defines spinodal for the formation of microphases. The structural parameters were set as $n_t = 30$, $\delta t = 3$, and $n_m = 25$.

SCLCP chain is not influenced by the backbone or the spacer.

The spinodal curves for the isotropic-microphase instabilities are shifted towards higher temperatures as the degree of polymerization increases. According to Finkelmann ad Rehage [27], this behavior is well established experimentally, and can be understood by the restriction of the translational and rotational motions of the mesogenic molecules due to the linkage to the backbone. After $n_t \approx 10$, the chain length is such that there is no correlation between the first monomer in the chain and the last added. Therefore, the instability curve is hardly affected by the polymerization degree.

The spinodal curve IM is also influenced by the ratio $\frac{\omega}{\chi}$, specially in the rod-rich regions, as can be seen comparing phase diagrams (a) and (b) of figure 2. However, this dependence vanishes with increasing n_t and after $n_t = 5$ the spinodal curve IM is not longer affected by the ratio $\frac{\omega}{\chi}$.

C. Characteristic length

In figure 3, we show the value of q^* that defines the spinodal curve IM as a function of the rod volume fraction. The solid line is the wave vector for the length of the rod-coil part of the SCLCP, i.e. $q_{rs} = \frac{2\pi}{n_r + \sqrt{\frac{n_s}{6}}}$. As it can be seen from the figure, even in the rod-rich region, the modulation period of the microphase is determined by both rod length and spacer conformation. Nevertheless, up to $f_r \approx 0.8$, q^* is always smaller than q_{rs} . As the polymerization degree is increased (see dotted and dashed lines in figure 3), this difference increases. On the basis of this information and the experimental data on SCLCP discussed by Noirez and coworkers in references [28][29][30], we suggest the microphase region is formed by structures in which the backbone is confined

between layers containing the rigid cores. Therefore, the difference between q^* and q_{rs} might be attributed to the conformation of the backbone.

D. Temperature equivalence

So far, all the information we have discussed is based on the calculation of the Flory-Huggins parameters as a function of the structural parameters of the model and the ratio $\frac{\omega}{\chi}$. Since it is well known that the Flory-Huggins parameter has a dependence on the inverse of temperature of the form

$$\chi = \frac{A}{T} + B, \quad (19)$$

it is interesting to relate the constants A and B to the SCLCP chemical constitution in order to give a more realistic characteristic to our results.

From thermodynamic arguments applied on the Flory's lattice model for a polymer in a solvent, it can be shown that the temperature dependent term of expression (19) is the enthalpic contribution from rearrangement of the contacts polymer-polymer, solvent-polymer and solvent-solvent. See for example reference [23] for a review on this subject. This term can be estimated using the Hildebrand solubility parameters of the polymer and the solvent segments. Following [31], the enthalpic contribution to the Flory-Huggins parameter is

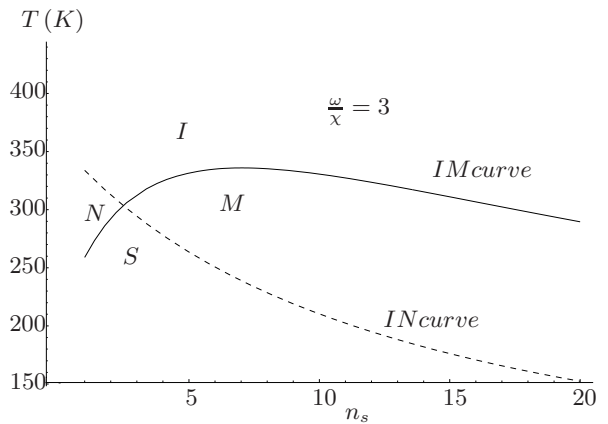
$$A = \frac{V_{seg}}{R} (\delta_{pol} - \delta_{solv})^2, \quad (20)$$

where the δ 's are the Hildebrand solubility parameters of each component of the mixture, V_{seg} is the common segment volume and R is the ideal gas constant. The Hildebrand solubility parameters are approximated through the relationship with the cohesive energy and the group contribution method [31].

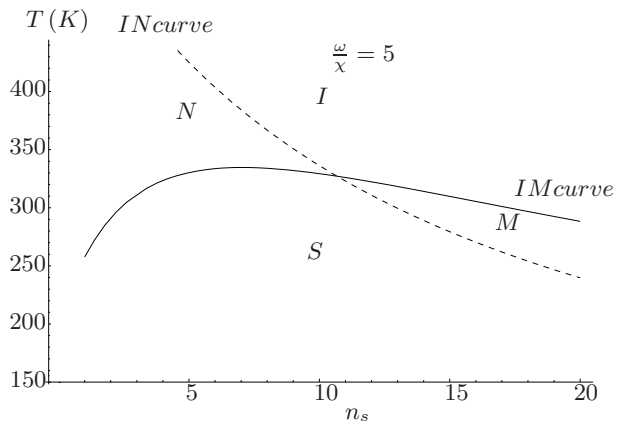
The athermal term in expression (19) is related to internal degrees of entropy of the polymers. According to different authors it might have its origin in features such as conformational asymmetries of the components of the mixture [32, 33] and nematic interaction between the segments originated by the flexibility differences between the polymers. In general, this term is determined empirically[34].

This equivalence between temperature and the χ parameter allows us to compare our results with experimental data available in literature. As an example, in appendix B we calculated the Flory-Huggins parameter as a function of temperature for the polyacrylates shown in figure 6, with $n_s = 2$, $n_t = 30$, $\delta t = 2$ and $n_r = 9$.

This SCLCP has a isotropic-nematic transition at $T_{IN}^{exp} = 425K$ [27]. As a test for the validity of this correspondence between temperature and χ parameter,



(a)



(b)

Figure 4: Transition temperatures as a function of the spacer length. Parameters: $\delta t = 3$, $n_r = 10$, $n_t = 30$

we calculated the transition temperature for this polymer using our model. Setting $\frac{\omega}{\chi} = 4.6$ and $B = -0.05$ we obtain a critical temperature of $T_{IN}^{teo} = 430K$. Since we have done several approximations in the model, and the results depend on two adjustable parameters, we must not be too optimistic about the agreement of the model presented here with respect to the experimental data. Nevertheless, the agreement achieved can be considered as a good indicative of the possibility that main physical features of the systems are present in our phenomenological model.

From now on, we will use relation (19) to talk about temperature instead of the Flory-Huggins parameter. In this way our discussions will have a more intuitive background.

E. Influence of the structural parameters on the phase diagram morphology

According to Finkelmann and Rehage [27], the schematic phase behavior of SCLCP follows the same trends as low molar mass liquid crystals. For a fixed

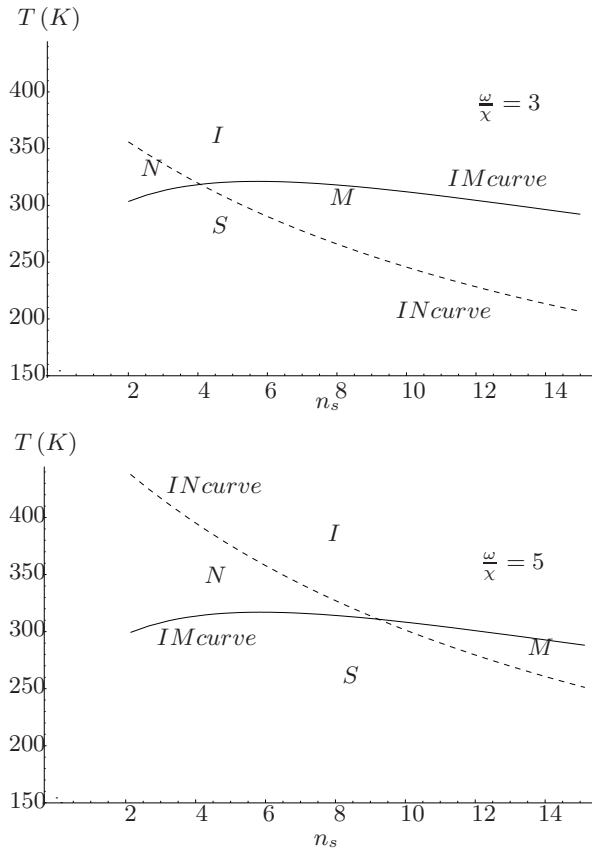


Figure 5: Transition temperatures as a function of the spacer length. Parameters: $\delta t = 5$, $n_r = 10$, $n_t = 30$.

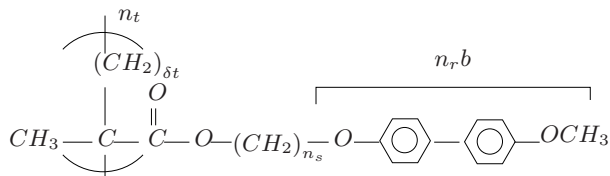


Figure 6: Polyacrylate used as example to calculate the dependence of χ on temperature.

mesogen length, increasing the length of the flexible spacer or the length of the backbone segment neighboring side chains decreases the instability temperature towards nematic or smectic mesophases. Some aspects of our results are however different. First, in our model, for a fixed δt , the smectic phase is favored as n_s is increased only if $\omega < \omega_c$. Here, ω_c is a function of the isotropic-microphase transition temperature curve. It is defined as the curve ω_c that crosses the curve IM at the point at which it starts decreasing with increasing n_s . For larger Maier-Saupe couplings the general trend is opposite to that related by Finkelmann and Rehage. In figure 4 we show the phase diagram as a function of the spacer length for two different values of $\frac{\omega}{\chi}$. In the first case, the behavior is as described by Finkelmann and Rehage, while in the second case, where the $\frac{\omega}{\chi}$ ratio is larger, the smectic

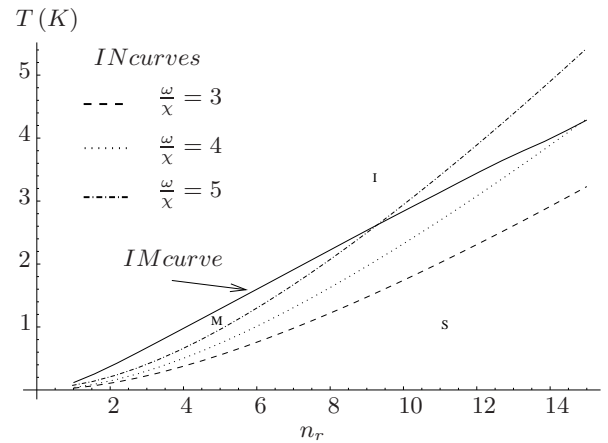


Figure 7: Transition temperatures as a function of the mesogen length. The parameters were set as $\delta t = 3$, $n_s = 10$, $n_t = 30$.

phase is not necessarily favored by increasing n_s . In figure 5 we show the phase diagrams for a larger value of δt . As it can be deduced from the figure, the behaviors described above are maintained despite the larger value of δt .

As discussed by Auriemma[15] et al. and by Finkelmann and Rehage [27], another characteristic behavior of low molecular weight liquid crystals and enhanced in SCLCP, is the increase of the isotropization temperature with increasing length of the mesogenic groups. This trend is also present in our model. In figure , we show the transition temperature as a function of n_r for different values of the ratio $\frac{\omega}{\chi}$. In this case, the smectic phase is favoured by both the increase of n_r the interaction ratio $\frac{\omega}{\chi}$.

F. Microphase segregation

As mentioned before, an important feature of our model, is the possibility of microphase segregation besides the formation of nematic and smectic phases. In this sense, our phase diagrams for SCLCP are more similar to rod-coil diblock copolymers phase diagrams. In these systems, the mutual repulsion of the blocks, due to the difference in chain rigidity, and the constrains imposed by the connectivity of the blocks result into the formation of supramolecular structures as small as few nanometers[2]. If we think about the SCLCP as being a polymer in which the monomeric units are rod-coil diblock copolymers, it is quite natural to expect the existence of such microphases.

This kind of interplay between liquid crystalline mesophases and microstructure domains is documented experimentally for SCLCP made of diblock copolymers, as in references [35][36]. In these SCLCP, the repeated unit is a homogeneous diblock copolymer with a liquid-

crystalline monomer grafted to one of the blocks. Such kind of SCLCP exhibit microdomains with spherical, hexagonally packed cylindrical and lamellar structure. The morphology of their phase diagram can be related to the molecular weight, the block composition and the χ parameter.

Therefore, the existence of microphases in SCLCP is a possibility that should be considered when performing experiments and analyzing experimental data.

It is worth to note that despite our model predicts microphase segregation for SCLCP with certain structural characteristics, we can not differentiate the symmetries of this microphases. To distinguish between the different possible symmetries, it would be necessary to perform calculations with higher order terms of the free energy, as done by Reenders et al. [7] for the case of rod-coil diblock copolymers.

G. Frank elastic constants

As explained in the review written by Stephen and Straley[20], the gradient terms in Q of the free energy (13) are related to the Frank elastic constants.

The usual expression for the Frank elastic energy in terms of the director \mathbf{n} is

$$F_{elastic} = \frac{1}{2}K_1(\nabla \cdot \mathbf{n})^2 + \frac{1}{2}K_2(\mathbf{n} \cdot \nabla \times \mathbf{n})^2 + \frac{1}{2}K_3(\mathbf{n} \times \nabla \times \mathbf{n})^2. \quad (21)$$

The constants K_i are the splay, twist and bend Frank elastic constants. In general, the bending constant K_3 is larger than the other two, which are about the same order of magnitude. In many cases equation (21) is too complex to be of practical use. Thus, it might be useful consider all the constants as equal. In that case the elastic energy is reduced to

$$F_{elastic} \approx \frac{1}{2}K \partial_i n_j \partial_j n_i, \quad (22)$$

where the sum over repeated indexes is employed.

Equation (22) is not quantitatively correct but gives a qualitative idea of the distortions in nematic liquid crystals [37].

In figure 8 we show the correlation function for the nematic tensor calculated near the isotropic-nematic transition temperature. This correlation function can be approximated by a function of the kind

$$G_{QQ}(q) \approx \frac{1}{\mu + Lq^2}. \quad (23)$$

The inverse of G_{QQ} corresponds to the expansion of the free energy term proportional to the square of the nematic order parameter in power series of the wave vector.

$$G_{QQ}(q) \times 10^3$$

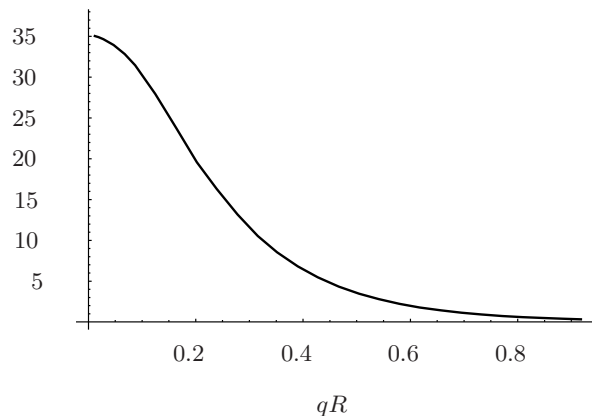


Figure 8: Correlation function for the nematic tensor calculated for $\delta t = 3$, $n_s = 7$, $n_r = 10$, $n_t = 30$, $\frac{\omega}{\chi} = 4$ and $T = 1.1T_{crit}$.

The coefficient μ carries the dependence on the Maier-Saupe coupling. When $\mu = 0$, the correlation function diverges at $q = 0$. Therefore, μ is defined by the the IN curve given by equation (18),

$$\mu = \frac{5}{f_r^2} - \frac{2\omega}{3} \frac{N}{n_t}.$$

The coefficient L , which corresponds to

$$L = \frac{n_t \left[n_r^2 (137 + 28n_t) (n_s + \delta t)^2 + 220n_s (n_s^2 + 3n_s\delta t + 3\delta t^2) \right]}{7 \left[3n_r^2 (n_s + \delta t)^2 + 4n_s (n_s^2 + 3n_s\delta t + 3\delta t^2) \right]}, \quad (24)$$

depends only on the structural parameters $n_r, n_s, \delta t$, and n_t . Regarding to the form of (23), we can interpret the quantity $\xi_n^2 = \frac{L}{\mu}$ as a correlation length related to the

nematic ordering. Also, coefficient L is the gradient term of the free elastic energy and thus can be associated to the elastic constant K . Note that this elasticity is purely

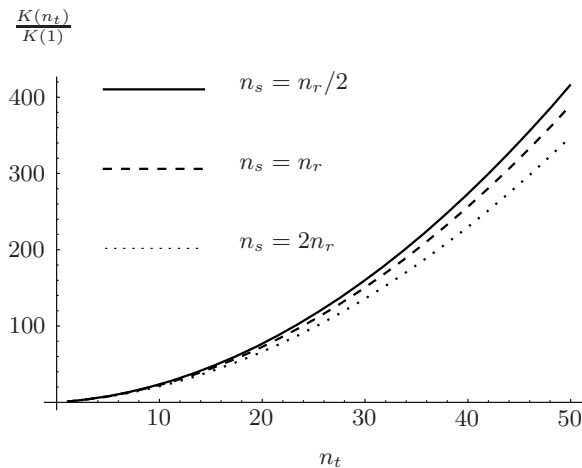


Figure 9: Elastic constant K as a function of the polymerization degree for various values of n_s at a temperature $T = 1.1T_{crit}$. The other parameters were set as $f_r = 0.4$, $\delta t = 3$, $\frac{\omega}{\chi} = 4$, $n_t = 30$.

entropic. Therefore, by studying the behavior of the correlation function G_{QQ} with the degree of polymerization and the structural parameter of the SCLCP, it's possible to obtain information of how the polymerization degree and the size of the spacer affect the nematic ordering.

In figure 9 we show the coefficient K as a function of the polymerization degree for various values of n_s near the isotropic-nematic transition temperature. Clearly, the additional correlations introduced by polymerization degree raise the energy cost of the nematic distortions. This reflects as a rise of the nematic correlation length. From (24) it is clear that K has an asymptotic behavior of n_t^2 . Therefore the nematic correlation length scales as n_t . While in low molar mass liquid the elastic energy represents a small fraction of the overall energy [37], its contribution can be amplified considerably by the polymerization in SCLCP.

On the other hand, the increase of the spacer size slightly reduces the value of K . The longer the spacer, the weaker the coupling between the mesogens and backbone conformation and the shorter the nematic correlation length.

H. Correlation length for the density fluctuations

Information about the correlation length can be extracted from the volume fraction correlation function in the reciprocal space, $G_{\phi\phi}(q)$. This function is calculated as the first element of the inverse of matrix $\Gamma^{(2)\mu\nu\rho\sigma}$. In figure 10 we show $G_{\phi\phi}(q)$ for different temperatures. Even at very high temperatures, its maximum is always at $q^* \neq 0$, i.e., the homogeneous state is not the lowest free energy state. Therefore, we suppose that near the transition temperature, the correlation function $G_{\phi\phi}(q)$ is proportional to a function of the kind

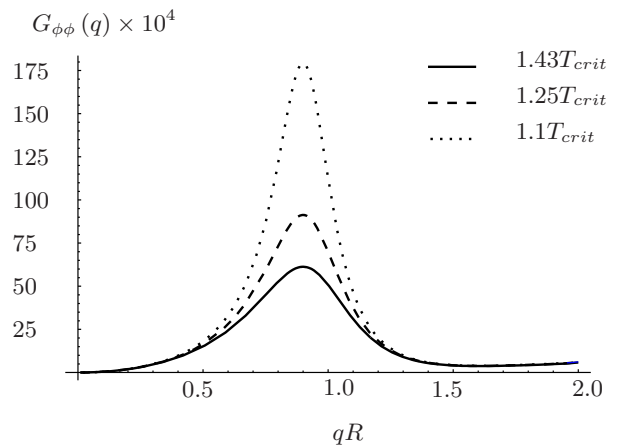


Figure 10: Volume fraction correlation function for temperatures close to the transition. The parameters used are $\delta t = 3$, $n_r = 10$, $n_s = 12$, and $\frac{\omega}{\chi} = 4$.

$$\mathcal{G}_{\phi\phi}(q) = \frac{1}{r + q^2 + \frac{u}{q^2}}.$$

For temperatures very close to the transition temperature, we can use the approximation

$$\mathcal{G}_{\phi\phi}(q) \approx \frac{1}{(q - q_0)^2 + \xi^{-2}}$$

where q_0 is the wave vector that maximizes $\mathcal{G}_{\phi\phi}(q)$, and ξ is the correlation length.

In figure we show the correlation length ξ as a function of the reduced temperature $t = \frac{T - T_c}{T_c}$ for different degrees of polymerization. The change in the value of the correlation length from $n_t = 1$ to $n_t = 2$ clearly shows the importance of the correlations induced by the linkage of the mesogens to the backbone. As the polymerization number increases, the correlation length increases. As discussed by Finkelmann and Rehage [27], after a certain number of monomers added to the SCLCP, the correlation between the last and the first monomer is lost.

As expected for a second order transition, the correlation length diverges at $t = 0$. Nevertheless, the form of the correlation function is such that all the allowed wave vectors form a spherical surface of radius q_0 . Such a condition is characteristic of systems with a fluctuation induced first order transition, as deduced by Brazovskii [38]. Higher order calculations would be necessary to corroborate this statement.

IV. CONCLUSIONS

As discussed above, the model we have proposed for SCLCP is in good agreement with the experimental observed trends discussed by Finkelmann and Rehage [27]

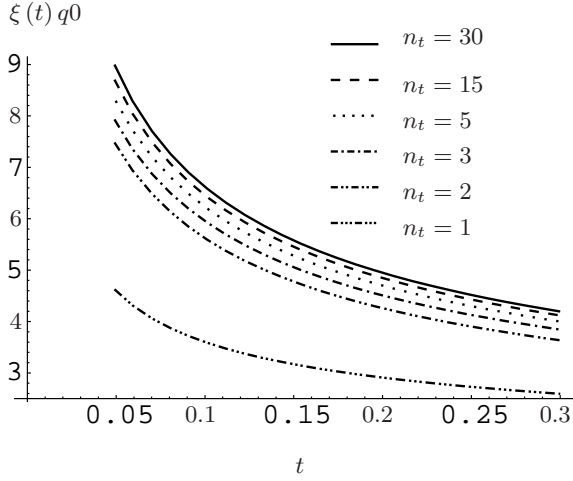


Figure 11: Correlation length as a function of the reduced temperature for different values of the polymerization degree. The parameters used are $\delta t = 3$, $n_r = 10$, $n_s = 12$, $\frac{\omega}{\chi} = 4$ and $n_t = 30$.

and Shibaev and Platé[1] for the transition temperatures of the SCLCP. Moreover, for an adequate value of the ratio $\frac{\omega}{\chi}$, our model predicts the existence of microphases with a modulated volume fraction but without orientational order. These microphases, originated from the mutual repulsion between the rigid and flexible blocks of the SCLCP, are already observed in SCLCP made of diblock copolymers as explained in references [35][36]. Nevertheless, further calculations are necessary in order to identify their symmetry.

As expected, the additional correlations introduced by the linkage of the mesogenic groups to a polymeric backbone through the flexible have a strong influence on the SCLCP critical behavior. This statement is supported by two main features. The first one is the swelling of the characteristic length of the microphase domains, that we have attributed to the backbone conformation. The second one is the influence of the spacer length n_s , and polymerization degree n_t on the phase diagram topology, correlation length of the volume fraction correlations and elastic energy associated to the nematic distortions.

Acknowledgments

M.H. thanks to FAPESP, project 03/06370-2, for financial support

H.W. thanks FAPESP and CNPq for financial support.

Appendix A: THE NONINTERACTING CORRELATION FUNCTIONS

The correlation functions are calculated as explained in references [7, 10], with the difference that there is a rigid rod attached at the end of each tooth of the comb polymer.

As an example, we calculate the correlation function rod-rod. This function has two contributions: one that comes from the correlation of the segments within the rod and the other one coming from the interaction between segments of two different rods. In this way:

$$\begin{aligned}
 G_{rr}(\mathbf{q}) &= \frac{1}{N^2} n_t \int_0^{N_r} d\tau \int_0^{N_r} d\tau' \langle e^{i(\tau-\tau')\mathbf{b}\cdot\mathbf{u}\cdot\mathbf{q}} \rangle \\
 &\quad + \frac{1}{N^2} e^{-2(qR_s)^2} \sum_{i \neq j}^{N_t} e^{-\frac{(qb)^2}{6} \delta t |i-j|} \int_0^{N_r} d\tau \int_0^{N_r} d\tau' \langle e^{i\tau\mathbf{b}\mathbf{u}^i \cdot \mathbf{q} + \tau'\mathbf{b}\mathbf{u}^j \cdot \mathbf{q}} \rangle \\
 &= f_r^2 \left[\frac{1}{n_t} K_{rr}(N_r b q) + e^{-2q^2 R_s^2} F_R(N_r b q)^2 \left(D_{n_t}(qR_b) - \frac{1}{n_t} \right) \right]. \tag{A1}
 \end{aligned}$$

where, $K_{rr}(x)$, $F_r(x)$ and $D_n(x)$ are the rod-rod correlation function, the form factor of a rod of length l and the Debye function for the backbone as explained in the text.

The other correlation function, calculated in the same way, are

$$G_{bb}(\mathbf{q}) = f_b^2 D_{n_b}(qR_b),$$

$$G_{ss}(\mathbf{q}) = \frac{f_s^2}{n_t} D_{n_s}(qR_s) +$$

$$f_s^2 F_{n_s}(qR_s)^2 \left(D_{n_s}(qR_b) - \frac{1}{n_t} \right),$$

where $F_{n_s}(qR_s) = \frac{1}{n_s} \left(\frac{1 - e^{-q^2 R_s^2}}{\frac{q^2 R_s^2}{e^{\frac{q^2 R_s^2}{n_s}} - 1}} \right)$ is the structure factor of the spacer,

$$\begin{aligned}
 G_{rs}(\mathbf{q}) &= f_r f_s F_r(qb n_r) F_{n_s}(qR_s) \\
 &\quad \times \left[\frac{1}{n_t} + \left(D_{n_t}(qR_b) - \frac{1}{n_t} \right) e^{-(qR_s)^2} \right]
 \end{aligned}$$

$$G_{rb}(\mathbf{q}) = 2f_r f_b \frac{6}{b^2 q^2} F_r(qbn_r) e^{-(qR_s)^2} \\ \times \left[1 - e^{\frac{1}{12} b^2 q^2 \delta t} F_{n_t}(qR_b) \right],$$

where $F_{n_t}(qR_b) = \frac{1}{n_b} \left(\frac{1 - e^{-q^2 R_b^2}}{e^{\frac{q^2 R_b^2}{n_b}} - 1} \right)$ is the structure factor of the backbone segments between two side groups,

$$G_{sb}(\mathbf{q}) = 2cf_b f_s F_{n_s}(qR_s) \frac{6}{b^2 q^2 n_b} \left[1 - e^{\frac{1}{12} b^2 q^2 \delta t} F_{n_t}(qR_b) \right],$$

where we have defined $\Delta^{\mu\nu} \equiv \frac{q^\mu q^\nu}{q^2} - \frac{\delta^{\mu\nu}}{3}$,

$$G_{Q_s}^{\mu\nu}(\mathbf{q}) = f_r f_s \Delta^{\mu\nu} F_{n_s}(qR_s) K_{Q_r r}(n_r b q) \\ \times \left\{ \frac{1}{n_t} + e^{-(qR_s)^2} \left[D_{n_t}(qR_b) - \frac{1}{n_t} \right] \right\},$$

$$G_{Q_b}^{\mu\nu}(\mathbf{q}) = f_r f_b F_{Q_r}(ql) e^{-(qR_s)^2} \frac{6}{b^2 q^2 n_b} \\ \times \left[1 - e^{\frac{1}{12} q^2 b^2 \delta t} F_{n_t}(qR_b) \right]$$

where $F_{Q_r}(x) = \frac{1}{2x^3} [3 \sin(x) - 3x \cos(x) - x^2 Si(x)]$ and $K_{Q_r}(x) = \frac{4x - x \cos x - 3 \sin x - x^2 Si(x)}{x^3}$ as defined in reference [7],

$$G_{Q_r}^{\mu\nu}(\mathbf{q}) = f_r^2 \Delta_{\mu\nu} \left[\frac{1}{n_t} K_{Q_r r}(ql) + e^{-2(qR_s)^2} \right. \\ \left. \times F_{n_r}(ql) F_{Q_r}(ql) \left(D_{n_t}(qR_b) - \frac{1}{n_t} \right) \right]$$

$$G_{QQ}^{\mu\nu\rho\sigma}(\mathbf{q}) = f_r^2 \sum_{i=1}^3 \mathcal{T}_i^{\mu\nu,\rho\sigma} \left[\frac{1}{n_t} K_{Si}^{(2)} \right. \\ \left. + e^{-2(qR_s)^2} F_{Q_r}(ql)^2 \left(D_{n_t}(qR_b) - \frac{1}{n_t} \right) \delta_{i,3} \right],$$

where the tensors $\mathcal{T}_i^{\mu\nu,\rho\sigma}$ and the functions K_{si} are defined as in reference [7].

Therefore, the correlations used to calculate matrix 11 are defined as follows:

$$G_{cr}(\mathbf{q}) = G_{rs}(\mathbf{q}) + G_{rb}(\mathbf{q}),$$

$$G_{cc}(\mathbf{q}) = G_{ss}(\mathbf{q}) + G_{bb}(\mathbf{q}) + 2G_{bs}(\mathbf{q}),$$

and

$$G_{Qc}(\mathbf{q}) = G_{Qs} + G_{Qb}.$$

Appendix B: THE HILDEBRAND PARAMETERS

According to reference [31], for non polar substances, the solubility parameter can be calculated through its relationship with the cohesive energy and its molar volume:

$$\delta = \sqrt{\frac{E_{coh}}{V}} \quad (B1)$$

Using to the group contribution method, the solubility parameter of a monomer unit is expressed as the sum of independent contributions from the atomic groups that constitute the unit,

$$E_{coh} = \sum_i E_{coh}^{(i)}. \quad (B2)$$

In the case of interest, we are considering the mixture of two components: the comb polymer (backbone and spacer). Therefore, it is convenient to choose the the segment unit as having a molar volume equivalent to that of the CH_2 . In this way, using (B1) and the with the data in reference is [31], we find that the Hildebrant solubility parameter for the flexible part of the polyacrylate is

$$\delta_{pol} = 16.13 (\text{Jcm}^{-3})^{1/2}.$$

For the rigid part, we must divide the cohesion energy of the whole group by n_r . This is equivalent to substitute the rigid rod by a chain of n_r units of CH_2 each one with a solubility parameter $\delta_{solv} = \sqrt{\frac{E_{rod}^{coh}}{n_r V}}$. In this way we obtain the Hildebrant solubility parameter for the rigid core,

$$\delta_{solv} = 7.73 (\text{Jcm}^{-3})^{1/2}.$$

By substituting and in δ_{pol} and δ_{solv} in 20, it is possible to calculated transition temperatures.

-
- [1] V. P. Shibaev and N. A. Platé, *Advances in Polymer Science* **60**, 173 (1984).
 [2] M. Lee, B. Cho, and W. Zin, *Chemical Review* **101**, 3869 (2001).

- [3] N. Yamazaki, M. Motoyama, M. Nonomura, and T. Ohta, *The Journal of Chemical Physics* **120**, 3949 (2004).
 [4] V. Pryamitsyn and V. Ganesan, *The Journal of Chemical Physics* **120**, 5824 (2004).

- [5] W. Renz and M. Warner, *Physical Review Letters* **56**, 1268 (1986).
- [6] H. Finkelmann, *Liquid crystallinity in Polymers* (New York: VCH Publishers Inc, 1991).
- [7] M. Reenders and G. ten Brinke, *Macromolecules* **35**, 3266 (2002).
- [8] M. Motoyama, N. Yamazaki, M. Nonomura, and T. Ohta, *Journal of the Physical Society of Japan* **72**, 991 (2003).
- [9] M. W. Matsen and C. Barrett, *The Journal of Chemical Physics* **109**, 4108 (1998), .
- [10] A. Shinozaki, D. Jasnow, and A. C. Balazs, *Macromolecules* **27**, 2496 (1994).
- [11] C. H. Vlahos and M. K. Kosmas, *J. Phys. A: Math. Gen.* **20**, 1471 (1987).
- [12] R. Wang, Z. Jiang, and J. Hu, *Polymer* **46**, 6201 (2005), .
- [13] A. R. K. Sergei V. Vasilenko, Valery P. Shibaev, *Die Makromolekulare Chemie* **186**, 1951 (1985), .
- [14] R. Matheson Jr and P. Flory, *Macromolecules* **14**, 954 (1981).
- [15] F. Auriemma, P. Corradini, and M. Vacatello, *The Journal of Chemical Physics* **93**, 8314 (1990).
- [16] X. J. Wang and M. Warner, *J. Phys. A: Math. Gen.* **20**, 713 (1987).
- [17] A. ten Bosch, P. Maissa, and P. Sixou, *The Journal of Chemical Physics* **79**, 3462 (1983), .
- [18] R. Holyst and M. Schick, *The Journal of Chemical Physics* **96**, 730 (1992).
- [19] W. Maier and A. Saupe, *Z. Naturforsch, Teil A* **15**, 287 (1960).
- [20] M. J. Stephen and J. P. Straley, *Reviews of Modern Physics* **46**, 617 (1974), .
- [21] A. M. Gupta and S. F. Edwards, *The Journal of Chemical Physics* **98**, 1588 (1993), .
- [22] A. J. Liu and G. H. Fredrickson, *Macromolecules* **26**, 2817 (1993).
- [23] I. Teraoka, *Polymer solutions* (Wiley New York, 2002).
- [24] C. Singh, M. Goulian, A. J. Liu, and G. H. Fredrickson, *Macromolecules* **27**, 2974 (1994).
- [25] T. A. Vilgis, *Physics Reports* **336**, 167 (2000).
- [26] P. G. de Gennes, *Scaling Concepts in Polymer Physics* (Cornell University Press Ithaca and London, 1979), .
- [27] H. Finkelmann and G. Rehage, *Advances in Polymer Science* **60**, 99 (1984).
- [28] L. Noirez, C. Boeffel, and A. Daoud-Aladine, *Physical Review Letters* **80**, 1453 (1998), .
- [29] L. Noirez, P. Keller, and J. Cotton, *Liquid Crystals* **18**, 129 (1995).
- [30] L. Noirez, P. Davidson, W. Schwarz, and G. Pepy, *Liquid Crystals* **16**, 1081 (1994).
- [31] E. Grulke, J. Brandrup, and E. Immergut, *Polymer handbook* (Wiley Interscience Publication , New York, 1998).
- [32] K. Almdal, M. Hillmyer, and F. Bates, *Macromolecules* **35**, 7685 (2002).
- [33] G. Fredrickson, A. Liu, and F. Bates, *Macromolecules* **27**, 2503 (1994).
- [34] A. Liu and G. Fredrickson, *Macromolecules* **25**, 5551 (1992).
- [35] K. LEE and C. HAN, *Macromolecules* **35**, 3145 (2002).
- [36] R. Ivanova, R. Staneva, S. Geppert, B. Heck, B. Walter, W. Gronski, and B. Stühn, *Colloid & Polymer Science* **282**, 810 (2004).
- [37] P. G. de Gennes and J. Prost, *The Physics of Liquid Crystals* (Clarendon, Oxford, 1993).
- [38] S. A. Brazovskii, *Zh. Eksp. Teor. Fiz* **68**, 175 (1975).